Organic Electron-Transfer Reactions: Complex Kinetics in the Thermal Back Reaction of 2,6- and 4,6-Disulfonated Leucothionine with Ferric Ion

Jorge Riefkohl, Lolita Rodriguez, Lorraine Romero, Gabriel Sampoll, and Fernando A. Souto*

Department of Chemistry and Center for Energy and Environment Research, University of Puerto Rico, Mayaguez Campus, Mayaguez, Puerto Rico 00708

Received June 26, 1985

The kinetics of the oxidation with ferric ion of 2,6- and 4,6-disulfonated leucothionines has been examined by stopped-flow techniques. Ortho-sulfonation of the dye form of thionine (D) has led to complex kinetics that can be interpreted in terms of association or ion-pair formation between ferric ion and the fully reduced leuco form (L) of the dye. The resulting effect is that association of the reagents, instead of facilitating the oxidation of L, becomes a trap since the final stages of the oxidation are a relatively slow process. Return to the colored form D is viewed to take place mostly by electron exchange between nonassociated species. The behavior of the coupled kinetic system (see Scheme II) can be rationalized in terms of competing electron transfer via k_{-2} and oxidation of L via k_{-3} either as the ligand within a metal complex or as the anion in an ion pair. The rate of oxidation depends on the degree of reorganization that the species involved must suffer during the act of electron transfer, and since oxidation of L involves flattening of the phenothiazine moiety, reduction of the associated species results in a highly unfavorable electron-transfer process. In contrast, the free hydrated ferric ion reacts with any of the sulfonated leucothionines at a faster rate than with the parent compound.

The study of the kinetics of photoinduced (forward) and thermal (backward) electron-transfer reactions between organic or organometallic redox dye species has attracted considerable attention in recent years. This is a result of the fact that natural and artificial photosynthetic schemes[1] rely both in efficient electron-transfer quenching[2] of molecular excited states[3] (primary electron transfer) and in favorable kinetics for the subsequent thermal back reactions (secondary electron transfer). A considerable number of studies with model photosynthetic systems have been reported dealing with the experimental characterization of the photophysical and photochemical events ensuing the act of light absorption.[4,5] The characterization of the kinetics of the corresponding thermal back reactions is, of course, of interest and has been pursued quite actively.[5]

Recently we have reported the synthesis and characterization of disulfonated thionines (2,6- and 4,6-DST), discussing in detail the ground state properties and the synthetic methodology for these compounds (Scheme I).[6] We have also studied the corresponding photochemical,[7a] photophysical,[7b] and photoelectrochemical[8] properties in the presence of added ferrous ions, the quencher. The results obtained have prompted us to examine the kinetics of the thermal oxidation by ferric ion of the fully reduced leuco forms of these compounds (LDST's). We have found that ortho-sulfonation of the parent compound results in complex kinetics that can be explained in terms of association or ion-pair formation between LDST's and Fe^{3+}. Invoking kinetic effects similar to those believed in operation when chelation of the reactants is involved,[9] the oxidation of L should have been facilitated by association with ferric ion, leading to faster electron-transfer kinetics.[10] However, in this case association of the reacting species leads to a trap since the oxidation of the reduced dye is a slow process. Return to the dye (D) takes place mostly by electron exchange between unassociated species.

Scheme I

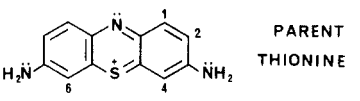

Scheme II

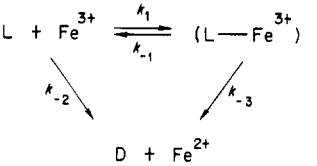

Results

Oxidation in the stopped flow of electrochemically produced parent L with excess Fe^{3+} gives in our hands a good pseudo-first-order behavior, showing in 50 mM H_2SO_4 perfectly linear plots of k_{obsd} vs. $[Fe^{3+}]$ (Figure 1a).[11]

(1) (a) Calvin, M. "Simulating Photosynthetic Quantum Conversion" *Photochemical Conversion and Storage of Solar Energy*; Connolly, J. S., Ed.; Academic: New York, 1981; Chapter 1, pp 1-26. (b) Kalyanasundaram, K.; Gratzel, M. *Photochem. Photobiol.* **1984**, *40*, 807-821. (c) Harriman, A. *Photochemistry* **1983**, *14*, 513-525. (d) Heller, A. *Science (Washington, D.C.)* **1984**, *223*, 1141-1148. (e) Bard, A. J. *J. Electroanal. Chem. Interfacial Electrochem.* **1984**, *168*, 5-20. (f) Wrighton, M. S. *Pure Appl. Chem.* **1985**, *57*, 57-68.

(2) Chibisov, A. K. *Prog. React. Kinet.* **1984**, *13*, 1-61 and references therein.

(3) Davidson, R. S. "The Chemistry of Excited Complexes: A Survey of Reactions" *Advances in Physical Organic Chemistry*; Gold, V., Bethell, D., Eds.; Academic: New York, 1983; Vol. 19, Chapter 1, pp 1-130.

(4) (a) Hall, D. O.; Rao, K. K. *Photosynthesis*, 2nd ed.; Arnold: London, 1976. (b) Calvin, M. *Photochem. Photobiol.* **1976**, *23*, 425-444. (c) Harriman, A. "The Role of Porphyrins in Natural and Artificial Photosynthesis" *Energy Resources through Photochemistry and Catalysis*; Gratzel, M., Ed.; Academic: New York, 1983; Chapter 6, pp 163-215. (d) Fendler, J. H. *Bioessays* **1984**, *1*, 165-167.

(5) Gratzel, M. "Molecular Engineering in Photoconversion Systems", in ref 4c, Chapter 3, pp 71-98.

(6) (a) Albery, W. J.; Bartlett, P. N.; Lithgow, A. M.; Riefkhol, J. L; Rodriguez, L. A.; Romero, L.; Souto, F. A. *J. Org. Chem.* **1985**, *50*, 596-603. (b) Lithgow, A. M.; Riefkohl, J. L.; Rodriguez, L. A.; Romero, L.; Souto, F. A. *J. Chem. Res., Synop.* **1984**, 352-353, *J. Chem. Res., Miniprint* **1984**, 3119-3130.

(7) (a) Souto, F. A. "Energy for the Americas" *Proceedings of the International Energy Conference*, Bonnet, J. A., Ed.; Pergamon: New York, 1986. (b) Riefkohl, J. L.; Rodriguez, L. A.; Romero, L.; Sampoll, G.; Souto, F. A., submitted for publication in *J. Phys. Chem.*

(8) (a) Albery, W. J.; Bartlett, P. N.; Foulds, A. W.; Souto, F. A.; Whiteside, R. *J. Chem. Soc., Perkin Trans. 2* **1981**, *77*, 794-800. (b) Riefkohl, J. L.; Rodriguez, L. A.; Romero, L.; Souto, F. A. *J. Electrochem. Soc.*, in press.

(9) Ashcroft, S. J.; Mortimer, C. T. *Thermochemistry of Transition Metal Complexes*; Academic: New York, 1970.

(10) Cotton, F. A.; Wilkinson, G. *Advanced Inorganic Chemistry*, 3rd ed.; Wiley: New York, 1972; pp 650-680.

0022-3263/86/1951-2468$01.50/0

Table I. Rate Constants[a] and Half-Wave Potentials[b] for Thionine and Its 2,6- and 4,6-Disulfonated Derivatives

	k_{-2}	$k_{-2} + k_1$	$k_{-1} + k_{-3}$	k_1	k_{-3}	k_{-1}	$E_{1/2}$
TH	135						201
2,6-DST	206	599	0.17	393	0.06	0.11	180
4,6-DST	447	596	0.15	149	0.05	0.10	158

[a] Bimolecular rate constants in $dm^3\ mol^{-1}\ s^{-1}$, unimolecular rates in s^{-1}. [b] Values of $E_{1/2}$ expressed in mV vs. SCE.

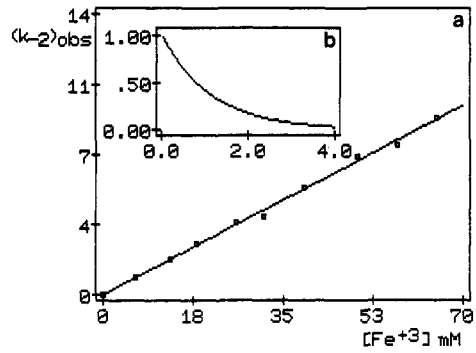

Figure 1. (a) Linear plot of observed rate constants (s^{-1}) vs. ferric concentration (mM) for the reoxidation of parent leucothionine. (b) Single exponential decay for the stopped-flow transient at 0.52 mM Fe^{3+} normalized as $(A_\infty - A_t)/(A_\infty - A_0)$.

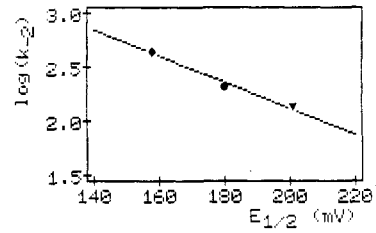

Figure 2. Hammett plot of log k_{-2} vs. $E_{1/2}$ (mV vs. SCE) showing the existence of a linear free energy relationship between redox potential and rate constants for thionine (▼), 2,6-DST (●), and 4,6-DST (◆).

Values for k_{obsd} were obtained by nonlinear, least-squares fitting of single exponentials to experimental transients normalized as $(A_\infty - A_t)/(A_\infty - A_0)$ (Figure 1b), finding in all cases excellent correlation. We estimate the bimolecular rate constant for this reaction ($[Fe^{3+}] = 0.520 - 65.0$ mM) to be of the order of 270 ± 10 ($k_L = 2k_{-2}$, $dm^3\ mol^{-1}\ s^{-1}$, 22.0 ± 0.1 °C), in good agreement with the value of 260 (22 °C) determined by Hatchard and Parker[12] using flash photolysis. In contrast, when the leuco form of 2,6- and 4,6-disulfonated thionine (LDST, 25 μM) is reacted in the stopped flow with Fe^{3+} (0.520 – 5.20 mM, H_2SO_4/Na_2SO_4, pH 1, ionic strength 0.2 M, 22.0 ± 0.1 °C) under pseudo-first-order conditions, only the initial part of the normalized absorbance transient can be described by a single exponential term. Recording the absorbance growth in the same time scale as for the parent thionine invariably leads to observed rate constants that have a decidely nonlinear variation with $[Fe^{3+}]$. Careful examination of the absorbance growth at faster and slower time scales reveals that the appearance of the dye occurs in two stages. For instance, with 0.520 mM Fe^{3+} there is a fast absorbance increase which is over in about 9 s but is followed by a much slower increase, reaching A_∞ in about 150 s. This biphasic behavior is typical of coupled kinetic systems[13] and can be explained by Scheme II, with LDST being associated reversibly with Fe^{3+} and oxidized[14] irreversibly to D, although naturally other possibilities exist. The kinetics of the initial phase corresponds to competition between association and oxidation of free L via k_1 and k_{-2}, respectively. The subsequent slower phase represents the oxidation of free and associated L in the free leuco/associated leuco mixture until only colored D remains.

In principle, one could obtain kinetic information about the LDST system by separately examining the absorbance of D in two appropriate time scales and fitting rate constants to the corresponding kinetic traces by nonlinear, asymptotic least-squares algorithms. However, our initial attempts in this direction failed, providing kinetic parameters for the slow and the fast phase that were out of bounds. In rigorous terms the kinetic analysis is more complex since the two stages are not at all separated, meaning that the rate constants in Scheme II, k_1 and k_{-2}, and k_{-1} and k_{-3}, respectively, are of the same order of magnitude, so that all processes are occurring simultaneously. The differential equations for this type of kinetic system have been solved.[13,15] The associated and the free L decay with curves that are the sum of two exponential terms, γ_1 and γ_2, with different preexponential factors, a and b, as described by eq 10 in the Appendix. The kinetic parameters γ_1 and γ_2 are apparent rates and do not represent actual rate consts. for individual components. Values for γ_1, γ_2, a, and b were obtained for different $[Fe^{3+}]$ by nonlinear, least-squares fitting a double exponential (Marquardt algorithm) to experimental transients normalized as $(A_\infty - A_t)/(A_\infty - A_0)$.[18] The actual rate constants for both isomers (Table I) were determined as we describe in detail in the Appendix for 2,6-DST that we take as a model.

Discussion

We find from the data in Table I that both isomers have virtually the same rate constants for dissociation (k_{-1}) and dye appearance from associated species (k_{-3}). The sum of the rate constants describing the decay of the corresponding leuco forms (LDST) is within experimental error also the same for both isomers. The main difference in the redox behavior of 2,6- and 4,6-DST lies in the distri-

(11) (a) Wildes, P. D.; Lichtin, N. N. *J. Phys. Chem.* **1978**, *82*, 981. (b) Hay, D. W.; Martin, S. A.; Ray, S.; Lichtin, N. N. *Ibid.* **1981**, *85*, 1474. (c) Osif, T. L.; Lichtin, N. N.; Hoffman, M. *Ibid.* **1978**, *82*, 1778. (d) Lichtin, N. N. "Photogalvanic Processes" *Solar Power and Fuels*; Bolton, J. R., Ed.; Academic: New York, 1977; Chapter 5, pp 133–135.

(12) Hatchard, C. G.; Parker, C. A. *J. Chem. Soc., Faraday Trans.* **1961**, *57*, 1093–1106. Also see Albery, W. J.; Bartlett, P. N.; Bowen, W. R.; Fisher, F. S.; Foulds, A. W. *J. Electroanal. Chem. Interfacial Electrochem.* **1980**, *107*, 23–35.

(13) (a) Capellos, C.; Bielski, B. H. J. *Kinetic Systems: Mathematical Description of Chemical Kinetics in Solution*; Wiley: New York, 1972; pp 73–75. (b) Seeman, J. I.; Farone, W. A. *J. Org. Chem.* **1978**, *43*, 1854–1864. (c) Rybak, W.; Haim, A. *J. Phys. Chem.* **1981**, *85*, 2856–2860. (d) Zuman, P.; Patel, R. C. *Techniques in Organic Reaction Kinetics*; Wiley: New York, 1984; pp 102–120. (e) McClelland, R. A.; Seaman, N. E.; Duff, J. M.; Branston, R. E. *Can. J. Chem.* **1985**, *63*, 121–128.

(14) The oxidation of leucothionine by ferric ion is a one-electron process, but since the resulting semithionine radical cation dismutates with high collisional efficiency (bimolecular rate about the same magnitude as the encounter frequency $\sim 6.8 \times 10^9\ dm^3\ mol^{-1}\ s^{-1}$), this step can be safely ignored for the present discussion.[7,12]

(15) Demas, J. N. *Excited State Lifetime Measurements*; Academic: New York, 1983, pp 59–69.

(16) (a) Marcus, R. A. *Annu. Rev. Phys. Chem.* **1964**, *15*, 155–196. (b) Sutin, N. *Prog. Inorg. Chem.* **1983**, *30*, 441.

(17) (a) Haim, A. *Prog. Inorg. Chem.* **1983**, *30*, 273. (b) Endicott, J. F.; Kumar, K.; Ramasami, T.; Rotzinger, F. P. *Ibid.* **1983**, *30*, 141.

(18) Balzani, V.; Scandola, F. "Light-Induced and Thermal Electron-Transfer Reactions", in ref 4c, Chapter 1, pp 39–42.

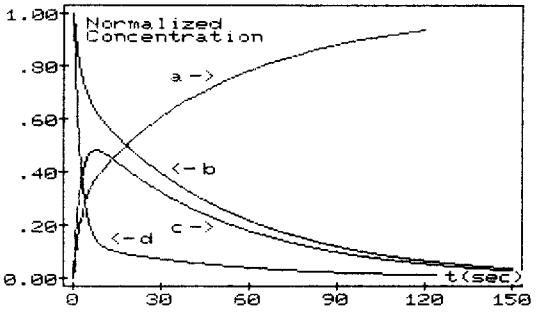

Figure 3. Variation with time of the coupled system at $[Fe^{3+}] = 0.52$ mM: (a) normalized absorbance at the λ_{max} of the dye $(A_t - A_0)/(A_\infty - A_0)$, (b) corresponding decay in terms of $(A_\infty - A_t)/(A_\infty - A_0)$, (c) calculated complex on ion pair concentration, (d) estimated concentration of free leuco.

Scheme III

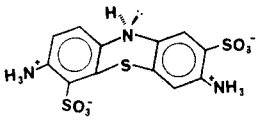

bution of this sum between the apparent rate of association (k_1) and that of the thermal back reaction (k_{-2}). The isomer with the sulfonates on the 4,6-positions reacts with ferric ion much faster than it can associate with it, while most of the free 2,6-analogue is removed from solution before it can react. Ortho-sulfonation of thionine clearly favors the association of its fully reduced leuco form with ferric ion since no such phenomena are observed for the parent compound. We attribute the differential behavior between 2,6- and 4,6-DST to the fact that 4,6-DST has stronger internal association by intramolecular hydrogen bonding between the amino and the sulfonic acid groups due to severe steric hindrance resulting from the proximity of the two sulfonic acid groups.[6,7] Intramolecular hydrogen bonding leads to a much higher energy of activation for external association with ferric ion for the 4,6- than for the 2,6-isomer, the sulfonates on the 2,6-isomer being much freer to interact with external cations.

The thermal back reaction of the free LDST's with ferric is for both isomers faster than for the parent thionine. This is an undesirable feature for this type of derivative that has its origin in the existence of a linear free energy relationship between redox potential and the rate of electron transfer (Table I). Figure 2 illustrates with data from the present study that this is the case. Exceptions to the linear free energy relationship are desirable from the point of view of energy conversion arrangements but are hard to find.

Figure 3 shows the observed and calculated concentration–time profiles for the 2,6-LDST/ferric system at $[Fe^{3+}] = 0.520$ mM. The behavior observed can be rationalized in terms of competing oxidation between free (k_{-2}) and associated species (k_{-3}), either in an ion pair or within a precursor complex, the latter leading to a successor complex that would eventually dissociate into products.[16,17] The rate of oxidation depends, among other factors, on the degree of reorganization that the species involved must suffer during the act of electron transfer and, since the oxidation of leucothionine involves flattening of the phenothiazine moiety (Scheme III) to give the planar semireduced quinone form, reduction of the associated Fe^{3+} results in highly unfavorable electron-transfer processes. In contrast, the free hydrated ferric ion reacts with the free LDST's at a faster rate than does the parent L ($k_L = 2k_{-2}$, in $dm^3\ mol^{-1}\ s^{-1}$ 270 for thionine, 412 for 2,6-DST, and 894 for 4,6-DST at 22.0 ± 0.1 °C).

Conclusions

The results reported offer one good example in which electron transfer is not the only process that can take place when a charged organic redox species react with inorganic redox species of opposing charge: ion pairing or other kind of association between the two species can be a competing step that can lead to faster overall reaction. In this case, however, association results in considerable retardation for electron transfer, implying that it is viable to find practical exceptions to the linear free energy relationship between redox potential and thermal back reaction rate constants. This possibility for the fully reduced, leuco forms of the disulfonated thionines upon mixing with concentrated solutions of ferric ion was difficult to predict on the basis of experimental evidence available in the literature when we initiated our studies. The only results available[8a,11,12] pointed out to the likelihood of the formation of successor-type complexes between the two reacting species, disregarding the possibility of ion pairing or the formation of precursor-type complexes between leucothionine and ferric ion. Theoretically, this fate for the LDST's could not be readily predicted either since the field of electron-transfer processes has been traditionally associated to inorganic reactions, and thus most of the theoretical background[16] and the supporting experimental evidence[17] is mainly based on reactions between spheric metal ions in aqueous solution. The fruitful interplay between theory and experiment observed for inorganic redox reactions does not have parallel in organic chemistry. The establishment of reactivity rules for organic redox reactions is of interest from the point of view of the transduction of light energy by the electron-transfer quenching of excited states[18] and the understanding of biological electron transfer.[19] Further work in these two directions is in progress.

Experimental Section

General Experimental Techniques. All experiments were performed in 0.1 N aqueous H_2SO_4 under anaerobic conditions at 22 ± 0.1 °C. A Perkin-Elmer Lambda 3B spectrophotometer was used for electronic absorption measurements. Path lengths of 0.1, 1.0, and 10 cm were used depending on dye concentration and absorbance. Stopped-flow experiments were carried out in an AMINCO-MORROW stopped-flow apparatus fitted to an AMINCO DW-2a high-performance spectrophotometer interfaced to an eight-channel Bascom-Turner 8120 digital data station and to an Apple //e microcomputer. The transient absorbance response of the spectrophotometer upon mixing in the stopped flow was recorded on trigger and processed with the Bascom/Apple system. The sampling interval was determined by the speed of the fast phase, with the slow phase then being compressed for analysis.

Electrochemical experiments were carried out with a Pine Instruments Co. rotating disc electrode (Model AFDD40PT with Pt disc of radius $r_1 = 0.564$ cm) rotated by an ASRPD variable speed rotator and an ASR motor controller manufactured by the same company. The controlling electronics were provided by a Princeton Applied Research (PAR) electrochemistry system composed of M-173 potentiostat/galvanostat, M-176 current-to-voltage converter, and M-176 universal programmer. The glass electrochemical cells (Model XLRC 10 jacketed cell), the reference (Model C10 saturated calomel electrode, SCE) electrode, and the counter (Model PT 16 Pt wire with a sintered glass diaphragm or extension tube) electrode were supplied by Astra Scientific Co. The electrochemical cell was thermostated at 25.0 ± 0.1 °C with a HAAKE FS3 refrigerated circulating bath. The leuco form of each dye was generated by controlled potential electrochemical reduction of the dye form at the plateau of the corresponding

(19) Lithgow, A. M.; Romero, L.; Sanchez, I. C.; Souto, F. A.; Vega, C. A. *J. Chem. Res. Synop.*, in press; *J. Chem. Res. Miniprint*, in press.

Table II. Kinetic Parameters and Observed Rate Constants for the Oxidation of 2,6-LDST[a,b]

$[Fe^{3+}]$	a	b	γ_1	γ_2	$x + y$	$(k_{-2})_{obsd}$	$(k_1)_{obsd}$
0.52	0.30	0.71	0.41	0.02	0.43	0.13	0.13
1.30	0.28	0.73	1.14	0.03	1.17	0.34	0.67
2.60	0.33	0.67	1.52	0.05	1.57	0.53	0.86
3.90	0.30	0.70	2.68	0.06	2.73	0.84	1.72
5.20	0.32	0.68	3.24	0.07	3.30	1.08	2.05

[a] Ferric concentration in mM; rates γ_1, γ_2, $(k_{-2})_{obsd}$, $(k_1)_{obsd}$, k_{-1}, and k_{-3} in s^{-1}; bimolecular rate constants in $dm^3\ mol^{-1}\ s^{-1}$. [b] γ_1 plot (Figure 3a): $m = (k_{-2} + k_1) = 599$, $n = (k_{-1} + k_{-3}) = 0.17$. $(k_1)_{obsd}$ plot (Figure 3b): $k_1 = 405$. $(k_{-2})_{obsd}$ plot (Figure 3c): $k_{-2} = 206$, $k_1 = m - k_{-2} = 393$. γ_2 plot (Figure 4): $p = (nk_{-2} + k_1k_{-3})/(m + n) = 0.10$. $(k_{-1} + k_{-3}) = 0.17$. $k_{-3} = 0.06$, $k_{-1} = 0.11$.

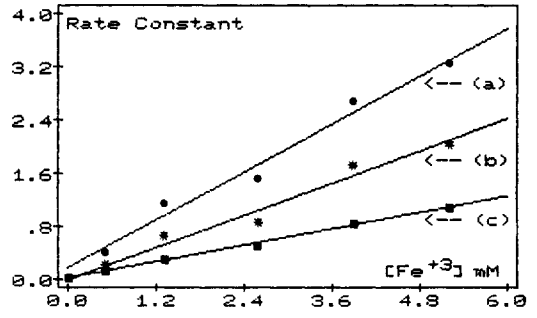

Figure 4. Plot of pseudo-first-order rate constants (s^{-1}) vs. ferric ion concentration (mM); (a) the apparent rate constant γ_1, (b) the rate of association $(k_1)_{obsd}$, (c) the rate of reoxidation of the free leuco form $(k_{-2})_{obsd}$.

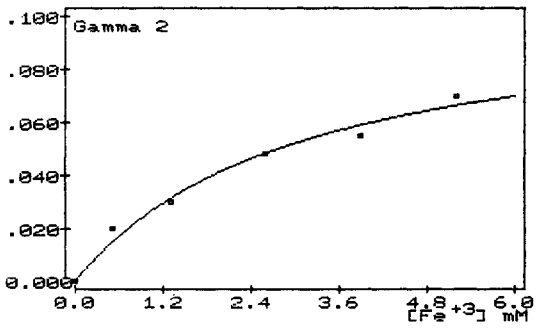

Figure 5. Michaelis curve fitting of the apparent rate constant γ_2 vs. ferric ion concentration.

current vs. voltage curves. A PAR coulometry cell system with Pt grid working and counter electrodes and an SCE reference electrode was quite readily adapted for this purpose. The solution containing the leuco form was transferred to the stopped-flow apparatus under anaerobic conditions by using gas tight syringes.

Chemicals and Solvents. The sulfonated thionine derivatives were prepared by direct sulfonation of the parent thionine with chlorosulfonic acid according to our published method.[6b,19] The procedures utilized for the analysis and isolation of the redox dyes are as described previously.[6a] The concentration of dye solutions (0.1 N aqueous H_2SO_4) was determined by spectrophotometric analysis in the visible of solutions diluted to the range of concentrations in which the Lambert–Beer law is obeyed.

All solvents were commercial grade and were used directly without further purification, with the exception of distilled water which was doubly distilled (DDW) for use as solvent for reactions and triply distilled (TDW, Milli-Q Super-Q Water Purification System) for chromatography, electrochemical experiments, and preparation of dye sample solutions. The sulfuric acid utilized was Ultrex grade supplied concentrated (18 M) by J. T. Baker Chemical Co. and was diluted with TDW. The ferric sulfate used was puriss. p.a. obtained from Fluka Chemical Co. The parent thionine utilized was supplied by Aldrich as the acetate and by the Allied Chemical Co. as the hydrochloride. All the inorganic reagents used meet ACS specifications and were supplied by either Fisher Scientific, Sigma, or Fluka. Sephadex G-25 Fine and Superfine and LH-20 and LH-60 gels obtained from Pharmacia Chemicals Co. were used for purification and desalting of the sulfonated derivatives. Prior to reaction in the electrochemical cell, the sulfonated dyes were subjected to cation-exchange chromatography on Bio-Rad Dowex resins (AG 50W-X2 or -X8, 200-400 Mesh, Na^+ form).

Acknowledgment. This work was carried out under contract with the U.S. Department of Energy (Office of Basic Energy Sciences, Contract DE-AS05-82ER12088). An Atlantic Richfield Foundation Grant of Research Corporation and research instrumentation grants awarded by the National Science Foundation (NSF Grants TFI-80-19833 and RII-83-05857) are acknowledged with appreciation. We are indebted to Professor W. John Albery for his encouragement and illuminating leadership and to Professors Georges G. Siegel, Albert Haim, and Manuel Rodriguez for helpful discussions.

Appendix

In this Appendix we describe the modus opperandi followed to obtain the rate constants for each isomer listed in Table I. We use throughout this discussion the 2,6-isomer as a model. The general kinetic system represented by Scheme II has been solved analytically. The general solution, described in detail in ref 13 and 15 (also see references therein), has been utilized in this work with the boundary value conditions that at $t = 0$, $[L] = [L]_0$, $[L\text{–}Fe^{3+}] = [C] = 0$, and $[D] = 0$, and at $t = \infty$, $[L] = 0$, $[C] = 0$, and $[D] = [L]_0$. The normalized concentrations of the leuco form, associated species or ion pair, and oxidized dye are then given by eq 1–3.

$$[L]/[L]_0 = g_1e^{-\gamma_1 t} - g_2e^{-\gamma_2 t} \quad (1)$$

$$[C]/[L]_0 = ((k_1)_{obsd}/(\gamma_1 - \gamma_2))(e^{-\gamma_2 t} - e^{-\gamma_1 t}) \quad (2)$$

$$[D]/[L]_0 = 1 - [L]/[L]_0 - [C]/[L]_0 \quad (3)$$

where

$$g_1 = (X_{obsd} - \gamma_2]/(\gamma_1 - \gamma_2) \quad (4)$$

$$g_2 = (X_{obsd} - \gamma_1)/(\gamma_1 - \gamma_2) \quad (5)$$

$$X_{obsd} = (k_{-2})_{obsd} + (k_1)_{obsd} \quad (6)$$

$$2\gamma_1 = (X + Y)_{obsd} + ((X - Y)_{obsd}^2 + 4(k_1)_{obsd}k_{-1})^{1/2} \quad (7)$$

$$2\gamma_2 = (X + Y)_{obsd} - ((X - Y)_{obsd}^2 + 4(k_1)_{obsd}k_{-1})^{1/2} \quad (8)$$

and

$$Y = k_{-3} + k_{-1} \quad (9)$$

According to this scheme, the normalized transient obtained from the growth of the absorbance of the dye at its λ_{max} is defined by eq 10, where $a = g_1 - ((k_1)_{obsd}/(\gamma_1 - \gamma_2))$

$$(A_\infty - A_t)/(A_\infty - A_0) = ae^{-\gamma_1 t} + be^{-\gamma_2 t} \quad (10)$$

and $b = -\{g_2 - ((k_1)_{obsd}/(\gamma_1 - \gamma_2))\}$. We find a, b, γ_1, and γ_2 for different $[Fe^{3+}]$ by Marquardt fitting a double exponential decay to the normalized experimental transients (Table II).

To determine the actual rate constants, in the first place, we obtain eq 11 from eq 4, 6, and 10

$$(k_{-2})_{obsd} = \gamma_2 + a(\gamma_1 - \gamma_2) \quad (11)$$

or from eq 5 instead of eq 4, we obtain eq 12

$$(k_{-2})_{obsd} = \gamma_1 - b(\gamma_1 - \gamma_2) \quad (12)$$

which allows to find k_{-2} as the slope of a $(k_{-2})_{obsd}$ vs. $[Fe^{3+}]$ plot (Figure 4c). In this manner, we obtain a value of 206 $dm^3\ mol^{-1}\ s^{-1}$ for k_{-2}. Secondly, we note in Figure 4a that the apparent rate constant γ_1 varies linearly with ferric ion, $\gamma_1 = m[Fe^{3+}] + n$, showing a steady increase in the range 0.520–5.20 mM (m = 599 $dm^3\ mol^{-1}\ s^{-1}$) and a small, but definitely nonzero, extrapolated intercept at $[Fe^{3+}]$ = 0 (n = 0.17 s^{-1}). This linear behavior of γ_1, first order in ferric, can be deduced from eq 7 considering that when $[Fe^{3+}]$ is small, γ_1 approaches Y, which can thus be identified as the intercept of the γ_1 vs. $[Fe^{3+}]$ plot. The small value observed for Y, and thus for k_{-1}, allows to neglect the term $4(k_1)_{obsd}k_{-1}$ in eq 7 at intermediate ferric concentrations, and, therefore, under those conditions, the slope of the γ_1 plot can be approximated by $(k_{-2} + k_1)$. This allows to obtain approximate values for $Y = (k_{-3} + k_{-1}) = n$ and $X = (k_{-2} + k_1) = m$ and in turn for $k_1 = X - k_{-2}$ = 393 $dm^3\ mol^{-1}\ s^{-1}$. The small value found for the intercept n permits to set a maximum value for k_{-3} of the order of 0.17 s^{-1}.

Third, equating the two square root terms in eq 7 and 8, we find the sum of the observed rate constants as

$$(X + Y)_{obsd} = \gamma_1 + \gamma_2 \quad (13)$$

which gives an expression for $(k_1)_{obsd}$ as

$$(k_1)_{obsd} = (\gamma_1 + \gamma_2) - Y - (k_{-2})_{obsd} \quad (14)$$

and yields a second estimate for k_1 as the slope of a $(k_1)_{obsd}$ vs. $[Fe^{3+}]$ plot (Figure 4b). The value of 405 $dm^3\ mol^{-1}\ s^{-1}$ found in this fashion compares very well with the value of 393 obtained from k_{-2} and the slope of the γ_1 plot.

Lastly, we obtain an estimate of the relative value of the first-order rate constants $k_{-3} + k_{-1}$ contained in Y, considering that the values of γ_2 are much smaller than those of γ_1 and show, instead of a linear behavior, a Michaelis-type dependence with ferric (Figure 5), $\gamma_2 = p[Fe^{3+}]/(q + [Fe^{3+}])$. Nonlinear least-squares fitting of the γ_2 values as a function of ferric concentration gives $p = (\gamma_2)_{max}$ = 0.10 s^{-1} and $q = [Fe^{3+}]_{1/2}$ = 3.0 mM. Evaluation of eq 8 as a function of $[Fe^{3+}]$ is in agreement with this observation since, for small $[Fe^{3+}]$, γ_2 vanishes, and, although the dependence with ferric is complex, we can show that the observed Michaelis behavior for the slow phase of this system can be deduced from the analytical expression for γ_2. Rearranging eq 8 gives eq 15.

$$\gamma_2 = \tfrac{1}{2}\{(X + Y)_{obsd} - ((X + Y)_{obsd}^2 - 4(Y(k_{-2})_{obsd} + (k_1)_{obsd}k_{-3}))^{1/2}\} \quad (15)$$

This equation can be expressed by a binomial expansion of the form

$$\gamma_2 = \{(Y(k_{-2})_{obsd} + (k_1)_{obsd}k_{-3})/(X + Y)_{obsd}\} + \{(Y(k_{-2})_{obsd} + (k_1)_{obsd}k_{-3})^2/(X + Y)_{obsd}^3\} + \ldots$$

The condition for the first term to be a good approximation for the series is that

$$\{(4Y(k_{-2})_{obsd} + (k_1)_{obsd}k_{-3})/(X + Y)_{obsd}^2\} \ll 1$$

and this is fulfilled under any of the two following circumstances: (a) $(k_1)_{obsd} \gg k_{-3}$ or (b) $(k_1)_{obsd} \gg k_{-1}$. In this fashion, at high ferric concentrations, we obtain eq 16 as an approximate expression for γ_2 consistent with the observed Michaelis behavior.

$$\gamma_2 = (Y(k_{-2})_{obsd} + (k_1)_{obsd}k_{-3})/(X + Y)_{obsd} \quad (16)$$

When $[Fe^{3+}]$ is large, $\gamma_2 \rightarrow p$ in $\gamma_2 = p[Fe^{3+}]/(q + [Fe^{3+}])$, and thus we can write eq 17

$$p = (Yk_{-2} + k_1k_{-3})/(X + Y) \quad (17)$$

which gives a value of 0.06 s^{-1} for k_{-3} and 0.11 s^{-1} for k_{-1}.

Inert Carbon Free Radicals. 7. "The (Kinetic) Reverse Effect" and Relevant Synthesis of New Monofunctionalized Triphenylmethyl Radicals and Their Nonradical Counterparts

Manuel Ballester,* Jaime Veciana, Juan Riera, Juan Castañer, Concepción Rovira, and Olga Armet

Instituto de Química Orgánica Aplicada (C.S.I.C.), C. Jorge Girona Salgado 18-26, 08034 Barcelona, Spain

Received November 14, 1985

The high chemical passivity of the so-called "inert free radicals" (IFRs), particularly those derived from perchlorotriphenylmethyl (PTM), has allowed one to ascertain the kinetic influence of the free radical character on the reactivity of their nonradical substituents. In all cases here reported (including homolysis of the carbon–halogen bond, nucleophilic substitutions, and radical-chain bromination), a moderate to dramatic increase of the reaction rates is observed. These results are accounted for in terms of transition-state stabilization by the radical character. In that connection, the following IFRs have been synthesized for the first time from other monosubstituted IFRs as immediate reaction precursors: methanol **15**, propionic acid **16**, bromomethane **18**, acetate **19**, tosylate **20**, diradical **21**, malonate **25**, propionyl chloride **26**, propionylalanine **27**, and chloromethane **29**. The nonradical compounds here described for the first time are bromomethane **2**, acetate **3**, tosylate **4**, iodomethane **5**, acetonitrile **6**, malonate **7**, acetamidomalonate **8**, methanol **9**, aldehyde **10**, acetic acid **11**, propionic acid **12**, chloromethane **13**, and propionylalanine **14**. Spectral (ESR, ^1H NMR, IR, UV–vis) and magnetic susceptibility data are reported.

The so-called "inert free radicals" (IFR) are trivalent-carbon species which are by far the most passive free radicals known.[1] A paradigm of an IFR is perchlorotriphenylmethyl (PTM).[1a] A significant number of

0022-3263/86/1951-2472$01.50/0